

Photoinduced electron transfer between acenaphthylene and 1,4-benzoquinones. Formation of dimers of acenaphthylene and 1 : 1-adducts and effect of excitation mode on reactivity of the charge-transfer complexes

2 PERKIN

Naoki Haga,^{*†a} Hiroaki Takayanagi^b and Katsumi Tokumaru^c

^a Department of Environmental and Natural Resource Science,
Tokyo University of Agriculture and Technology, Fuchu, Tokyo, 183-8509, Japan

^b School of Pharmaceutical Sciences, Kitasato University, Minato-ku, Tokyo, 108-8641, Japan

^c University of Tsukuba, Tsukuba, Ibaraki, 305-8577, Japan

Received (in Cambridge, UK) 3rd January 2002, Accepted 23rd January 2002

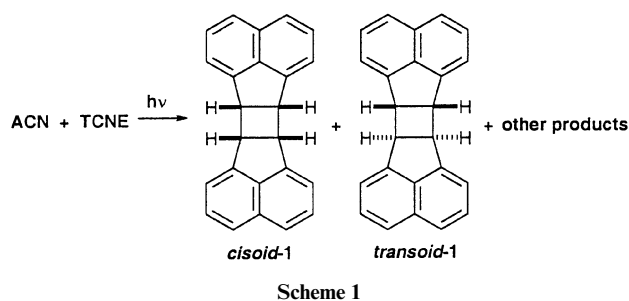
First published as an Advance Article on the web 20th February 2002

Photochemical reactions of acenaphthylene (ACN) with 1,4-benzoquinones (BQs) of varying reduction potentials in solution have been investigated in order to determine final products and quantum yields of the reactions and to get an insight into the factors which govern their reactivities. The products were the two isomeric dimers of ACN and three types of 1 : 1-adducts (cyclobutanes, furans, and oxetanes) between ACN and BQs. However, the product distribution varied widely with the substitution on the BQ skeleton. Two modes of excitation, that is, selective excitation of the charge transfer (CT) complex (*the CT mode*; typical wavelength: 546.1 nm) and direct excitation of ACN or BQs (*the direct mode*; typical wavelength: 435.8 nm), essentially gave similar product distributions when the reaction took place through both modes. However, *the direct mode* showed higher quantum yields for the reactions, $\Phi_{435.8}$, than *the CT mode*, $\Phi_{546.1}$. Moreover, $\Phi_{546.1}$ tended to increase with increase of free energy gap, $-\Delta G_{\text{BET}}$, between the ground state CT complexes and the resulting radical ion pair (RIP). These observations can be rationalized by a mechanism involving a distinctive RIP as an intermediate generated by photoinduced electron transfer in each mode. Thus, the solvent-separated radical ion pair (SSIP) produced in *the direct mode* excitation will undergo dissociation to the free radical ions (FRIs), $\text{ACN}^{+\cdot}$ and $\text{BQ}^{-\cdot}$, affording final products competing with backward electron transfer (BET). In contrast, the contact radical ion pair (CIP) produced in *the CT mode* excitation much more rapidly deactivates to the ground state than dissociates to FRIs *via* SSIP due to faster BET, whose rate depends on $-\Delta G_{\text{BET}}$. The 1 : 1-adducts can be formed from either a cage reaction inside the RIP (CIP or SSIP) or reaction between FRIs, whereas the dimers of ACN should be formed from reaction of $\text{ACN}^{+\cdot}$ with the ground state ACN.

Introduction

In the course of our mechanistic studies on the photochemical dimerization of acenaphthylene (ACN) in the presence of electron acceptors, characteristic features have been found for effect of wavelength of irradiation on the reactivity and the product distribution.^{1,2}

When TCNE was employed as an acceptor, direct excitation of ACN with light of wavelength longer than 420 nm (*the direct mode*) afforded two isomeric dimers of ACN (*cisoid-1* and *transoid-1*) as major products *via* the radical cation of ACN, $\text{ACN}^{+\cdot}$, in addition to a 1 : 1-adduct and two 2 : 1-adducts between ACN and TCNE in relatively low yields (Scheme 1).¹ On the other hand, selective excitation of the 1 : 1-charge-transfer (CT) complex between ACN and TCNE with light of wavelength longer than 500 nm (*the CT mode*) resulted in no reaction; however, irradiation of crystalline CT complex (ACN·TCNE) under the same wavelength of light gave the 1 : 1-adduct as the sole product.³ Mechanisms involving a distinct radical ion pair (RIP) rationalize the contrasting reactivity between the above two excitation modes. Thus, the solvent-separated radical ion pair (SSIP) generated from direct excitation of ACN and subsequent encounter with TCNE



dissociates to free radical ions (FRIs), $\text{ACN}^{+\cdot}$ and $\text{TCNE}^{-\cdot}$, leading to the final products, whereas the contact radical ion pair (CIP) generated from selective excitation of the CT complex readily deactivates to the ground state *via* very fast backward electron transfer (BET) preceding dissociation to the FRIs *via* the SSIP, especially when the free energy gap, $-\Delta G_{\text{BET}}$, between the ground state CT complexes and the resulting RIP is sufficiently small, as in the case of the ACN–TCNE system ($-\Delta G_{\text{BET}} = 120.8 \text{ kJ mol}^{-1}$). This is in keeping with the results of the transient spectroscopy by Mataga and his co-workers showing that CIPs produced by excitation of CT complexes of various aromatic hydrocarbons with nitriles or acid anhydrides tend to dissociate more rapidly with decrease of $-\Delta G_{\text{BET}}$.^{4,5}

To reveal the relationship between the reactivity of the excited state of the CT complexes leading to final (net) products

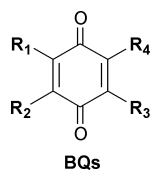
[†] Present address: Department of Environmental and Resource Science, Faculty of Agriculture, Tokyo University of Agriculture and Technology, 3-5-8, Saiwai-cho, Fuchu, 183-8509 Tokyo, Japan; Tel & Fax: +81-42-367-5617; E-mail: haga@cc.tuat.ac.jp

and $-\Delta G_{\text{BET}}$ of the resulting CIP, we have subsequently studied photochemical reactions of the CT complexes of ACN with a series of acceptors including nitriles, acid anhydrides, and 1,4-benzoquinones (BQs) with varying reduction potential ($E_{1/2}^{\text{Red}}$) of acceptors.² A clear trend has been revealed, namely that quantum yields for formation of net products by *the CT mode* tended to decrease with decrease of $-\Delta G_{\text{BET}}$, and finally became entirely non-reactive when $-\Delta G_{\text{BET}}$ was smaller than a threshold of *ca.* 160 kJ mol⁻¹. These results certainly indicate that dissociation from a CIP practically does not occur when $-\Delta G_{\text{BET}}$ is smaller than the above threshold, and dissociation from a CIP to FRIs *via* an SSIP tends to be accelerated with increase of $-\Delta G_{\text{BET}}$, therefore enhancing quantum yields for formation of net products.

We have noticed that irradiation of the CT complexes of ACN with a series of BQs as counterparts afforded 1 : 1-adducts between ACN as major products in addition to small amounts of the dimers **1**, whereas those with nitriles and acid anhydrides gave the dimers **1** as sole or major products.²

Consequently, a systematic study is required to reveal products and efficiency for net reactions on excitation of CT complexes employing a series of donor-acceptor systems. For this aim, BQs can be appropriate acceptors because their reduction potential ($E_{1/2}^{\text{Red}}$) can be varied by changing the substitution on the BQ skeleton.⁶

Our task in this study is as follows: (1) determination of product distribution between the dimers (*cisoid*- and *transoid*-**1**) and the 1 : 1-adducts between ACN and BQs on varying the substituents of BQs, (2) determination of quantum yields for formation of products both for *the CT mode* and for *the direct mode* excitation to compare the efficiency of the CIP with that of the SSIP in leading to final products, and (3) estimation of the quantitative relationship between $-\Delta G_{\text{BET}}$ and the reactivity. In this study, we have employed eleven kinds of BQs as listed in Scheme 2, covering a wide range of $E_{1/2}^{\text{Red}}$ from



- TMBQ ($R_1 = R_2 = R_3 = R_4 = \text{CH}_3$)
 2,5-DMBQ ($R_1 = R_3 = \text{CH}_3, R_2 = R_4 = \text{H}$)
 BQ ($R_1 = R_2 = R_3 = R_4 = \text{H}$)
 2-CBQ ($R_1 = \text{Cl}, R_2 = R_3 = R_4 = \text{H}$)
 2-BBQ ($R_1 = \text{Br}, R_2 = R_3 = R_4 = \text{H}$)
 2,5-DCBQ ($R_1 = R_3 = \text{Cl}, R_2 = R_4 = \text{H}$)
 2,6-DCBQ ($R_1 = R_4 = \text{Cl}, R_2 = R_3 = \text{H}$)
 TFBQ ($R_1 = R_2 = R_3 = R_4 = \text{F}$)
 TCBQ ($R_1 = R_2 = R_3 = R_4 = \text{Cl}$)
 TBBQ ($R_1 = R_2 = R_3 = R_4 = \text{Br}$)
 DDQ ($R_1 = R_2 = \text{CN}, R_3 = R_4 = \text{Cl}$)

Scheme 2

-0.84 V for duroquinone (TMBQ) to $+0.51$ V *vs.* SCE of 2,3-dichloro-5,6-dicyano-1,4-benzoquinone (DDQ).

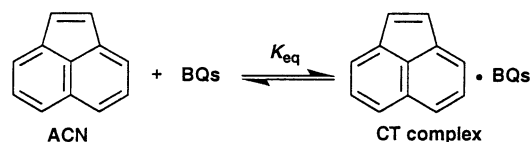
Results and discussion

Formation of CT complexes between ACN and BQs

Table 1 lists physical properties of the BQs employed including $E_{1/2}^{\text{Red}}$,⁶ the free energy change for photoinduced electron transfer from the singlet excited state of ACN to BQs, ΔG_{ET} ,⁷ ‡ triplet energies (E_{T}),^{8,9} and $-\Delta G_{\text{BET}}$.

‡ The free energy change, ΔG_{ET} , for ET from the excited singlet state of ACN to BQs can be calculated with values of oxidation potential ($E_{1/2}^{\text{Ox}}$) as 1.58 V⁴² (*vs.* SCE in AN) and excitation energy (ΔE_{excit}) as 257 kJ mol⁻¹²⁹ for ACN.

When ACN and BQs were mixed in dichloroethane (DCE) or acetonitrile (AN), vivid colors immediately developed except for 1,4-benzoquinone (BQ), 2,5-dimethyl-1,4-benzoquinone (2,5-DMBQ) and TMBQ owing to spontaneous formation of intermolecular CT complexes between them as shown in Scheme 3. The resulting CT complexes exhibited characteristic



Scheme 3

CT absorption in the region of 500–700 nm where neither ACN nor BQs showed absorption. § The coloration was varied among the substituents of the BQ. The mono-chlorinated derivative (2-CBQ) gave pale orange, and successive substitution by chlorine atoms progressively resulted in vermilion (TCBQ). When stored in the dark, these colored solutions persisted for more than a week and the components, ACN and BQs, could be quantitatively recovered intact from the mixture.

The equilibrium constants, K_{eq} , for formation of the CT complexes and their extinction coefficients, ϵ_{CT} , were determined spectrophotometrically¹⁰ as included in Table 1.

In the case of unsubstituted BQ, addition of ACN did not induce significant coloration, but slightly increased the absorbance in the region of 500–520 nm in DCE, showing formation of the CT complex. On the other hand, in the case of ACN–TMBQ, and ACN–2,5-DMBQ, no spectral change appeared even in concentrated solution as high as 2.0×10^{-1} M for both of the components. This indicates that these two BQs do not form the CT complex with ACN due to relatively low $E_{1/2}^{\text{Red}}$. ¶

Photochemical reaction by *the CT mode* and *the direct mode* in solution

To excite selectively the CT complexes, the CT absorption band of the complexes was irradiated with > 500 nm light (*the CT mode*) from a high pressure mercury lamp. Typically, an equimolar solution (2.0×10^{-2} M) of ACN and BQs in DCE was exposed to the light for 70 hours. Periodic TLC checking of the photolysate revealed simultaneous consumption of ACN and BQs and concurrent formation of products at conversions of ACN in the range of 8–38% except for the following unreactive combinations. Thus, ACN–TFBQ, ACN–TCBQ and ACN–DDQ were completely inert despite a relatively intense CT band at > 500 nm, and ACN–TMBQ and ACN–2,5-DMBQ, lacking CT absorption, were also inert under *the CT mode* irradiation.

All BQs used in this study and ACN exhibit absorption at 400–500 nm. Therefore, to excite directly BQs and ACN, irradiation was carried out with light of wavelength longer than

§ Because both ACN and BQs absorb significantly in the region of 400–460 nm, most of the CT bands except that of DDQ overlap with intensive absorption of ACN and BQs, and the λ_{max} of the CT complexes is missed.

¶ Photoinduced electron transfer between ACN and TMBQ will be exergonic when the excited singlet state of ACN participates, but be endoergonic with the triplet state of either ACN or TMBQ. ΔG_{ET} for the above processes is estimated⁷ as -11.2 , 49.8 and 29.8 kJ mol⁻¹, based on the following values: oxidation potential ($E_{1/2}^{\text{Ox}}$) of ACN, 1.58 V⁴² (*vs.* SCE in acetonitrile); reduction potential ($E_{1/2}^{\text{Red}}$) of TMBQ (-0.84 V *vs.* SCE);⁶ singlet triplet energy of ACN, 257²⁹ and 196 kJ mol⁻¹;³⁰ triplet energy of TMBQ, 216 kJ mol⁻¹.⁸ Similarly, ΔG_{ET} values for photoinduced electron transfer from either excited singlet or triplet state of ACN to the ground state 2,5-DMBQ are estimated as -25.8 and 35.2 kJ mol⁻¹, respectively, whereas that from triplet 2,5-DMBQ to ground state ACN is not available due to lack of data for triplet energy of 2,5-DMBQ.

Table 1 Free energy gap for electron transfer from ACN to BQs on excitation of ACN into the singlet excited state (ΔG_{ET}), free energy gap between the ground state CT complexes and the radical ion pair ($-\Delta G_{BET}$), excitation energy of the CT complexes (E_{CT}), CT absorption maxima (λ_{max}), formation constants (K_{eq}), and extinction coefficients (ϵ_{CT}) of the CT complexes of ACN with BQs in 1,2-dichloroethane, together with singlet energy (E_S), triplet energy (E_T), and redox potential ($E_{1/2}^{Red}$) of BQs

| Acceptor | E_S (A) ^a / kJ mol ⁻¹ | E_T (A) ^b / kJ mol ⁻¹ | $E_{1/2}^{Red}$ (A) ^c /V | ΔG_{ET} ^d / kJ mol ⁻¹ | $-\Delta G_{BET}$ ^e / kJ mol ⁻¹ | E_{CT} ^f / kJ mol ⁻¹ | λ_{max} ^g / nm | K_{eq} /M ⁻¹ | ϵ_{CT} /M ⁻¹ cm ⁻¹ |
|----------|--|--|--|--|--|---|--------------------------------------|---------------------------|---|
| TMBQ | — | 216 | -0.84 | -14.1 | 233.4 | — | — | — | — |
| 2,5-DMBQ | — | — | -0.67 | -25.8 | 221.6 | — | — | — | — |
| BQ | 262 | 224 | -0.51 | -45.9 | 201.7 | 238 | ^g | ^h | ^h |
| 2-CBQ | — | 223 | -0.34 | -62.3 | 185.3 | 226 | ^g | 1.85 (0.81) | 8 (3) |
| 2-BBQ | — | — | -0.325 | -63.8 | 183.8 | 217 | ^g | 2.52 (0.62) | 25 (8) |
| 2,5-DCBQ | — | 228 | -0.18 | -77.8 | 169.8 | 214 | ^g | 4.12 (0.62) | 46 (6) |
| 2,6-DCBQ | — | 221 | -0.18 | -77.8 | 169.8 | 214 | ^g | 3.28 (1.26) | 80 (40) |
| TFBQ | — | 228 | -0.08 | -87.4 | 160.2 | 210 | ^g | 3.06 (0.86) | 270 (50) |
| TCBQ | — | 228 | 0.01 | -96.1 | 153.4 | 203 | ^g | 4.15 (0.19) | 200 (30) |
| TBBQ | — | — | 0.00 | -95.2 | 152.4 | 194 | ^g | 4.28 (0.22) | 230 (30) |
| DDQ | — | — | 0.51 | -144.4 | 103.2 | 150 | 564 | 3.56 (0.41) | 4880 (1060) |

^a From ref. 8. ^b From refs. 8, 9. ^c From ref. 6. Values vs. SCE in MeCN. ^d Calculated⁷ with values of oxidation potential ($E_{1/2}^{Ox}$) as 1.58 V⁴² (vs. SCE in AN) and excitation energy (ΔE_{excit}) as 257 kJ mol⁻¹²⁹ for ACN. ^e Free energy gap between the ground state CT complexes and the radical ion pair ^f Estimated from the bottom edge of the CT absorption spectra. ^g The λ_{max} of the CT complexes are concealed among the intensive absorption of ACN and BQs, and therefore were not determined. ^h K_{eq} and ϵ_{CT} could not be determined due to too weak absorption of the CT complex.

Table 2 Product distribution of photochemical reactions between ACN and BQs in 1,2-dichloroethane^a

| Acceptor | Irradiation mode ^b | Conversion (%) ^c | Yield (%) ^d | | | | |
|----------|-------------------------------|-----------------------------|------------------------------|---------------------------|---------|----------------|----------------------|
| | | | 1 (<i>cisoid/transoid</i>) | 2 | 3 | 4 | Others |
| TMBQ | Direct | 94 | 20 (0.70) | 77 (2a) | 0 | 0 | 0 |
| 2,5-DMBQ | Direct | 72 | 25 (0.70) | 0 | 38 (3b) | 0 | 0 |
| BQ | Direct | 85 | 13 (2.5) | 0 | 0 | 19 (4c) | 0 |
| BQ | CT | 8 | 12 (2.6) | 0 | 0 | 32 (4c) | 0 |
| 2-CBQ | Direct | 94 | 11 (4.0) | 18 (5a) | 9 (3d) | 26 (4d) | 0 |
| 2-CBQ | CT | 20 | 16 (4.3) | 13 (5a) | 10 (3d) | 22 (4d) | 0 |
| 2-BBQ | Direct | 74 | 18 (3.2) | 18 (2e and 5a) | 0 | 4 (4e) | 0 |
| 2-BBQ | CT | 20 | 21 (4.5) | 23 (2e and 5a) | 0 | 9 (4e) | 0 |
| 2,5-DCBQ | Direct | 96 | 11 (2.8) | 29 (5b) | 25 (3f) | 0 | 0 |
| 2,5-DCBQ | CT | 18 | 4 (5.8) | 30 (5b) | 24 (3f) | 0 | 0 |
| 2,6-DCBQ | Direct | 89 | 19 (3.1) | 30 (2g and 5b) | 0 | 0 | 0 |
| 2,6-DCBQ | CT | 25 | 16 (4.4) | 36 (2g and 5b) | 0 | 0 | 0 |
| TFBQ | Direct | 55 | 25 (5.8) | 0 | 11 (3h) | 0 | 0 |
| TFBQ | CT | 0 | 0 | 0 | 0 | 0 | 0 |
| TCBQ | Direct | 82 | 10 (2.9) | 9 (2i) (6.5) ^e | 0 | 0 | 33 (7a), 39 (7b) |
| TCBQ | Direct | 81 | 7 (2.6) | 7 (2i) (7.2) ^e | 0 | 0 | 70 (8a) ^f |
| TCBQ | Direct | 70 | 8 (3.4) | 5 (2i) (6.6) ^e | 0 | 0 | 73 (8b) ^g |
| TCBQ | CT | 0 | 0 | 0 | 0 | 0 | 0 |
| TBBQ | Direct | 80 | 10 (2.2) | 8 (2j) | 32 (3j) | 16 (4j), 5 (6) | 0 |
| TBBQ | CT | 38 | 7 (2.6) | 12 (2j) | 50 (3j) | 20 (4j), 5 (6) | 0 |
| DDQ | Direct | 100 | 22 (5.8) | 0 | 0 | 0 | 0 |
| DDQ | CT | 0 | 0 | 0 | 0 | 0 | 0 |

^a [ACN] = 0.02 M, [BQs] = 0.02 M in dichloroethane under an argon atmosphere. ^b Irradiation mode: > 420 nm (direct); > 500 nm (CT). ^c Converted ACN after 24 hours (direct) and 70 hours (CT) of irradiation. ^d Yields based on ACN consumed. ^e *cisoid/transoid* ratio in parentheses. ^f Treatment with methanol after irradiation. ^g Treatment with ethanol after irradiation.

420 nm (*the direct mode*).|| By *the direct mode*, all of the ACN–BQ systems, including those which were unreactive by *the CT mode*, were converted to products. In general, when an equimolar (2.0×10^{-2} M) solution of ACN and BQs in DCE was irradiated for 24 hours, 55–100% of ACN disappeared with concurrent formation of reaction products.

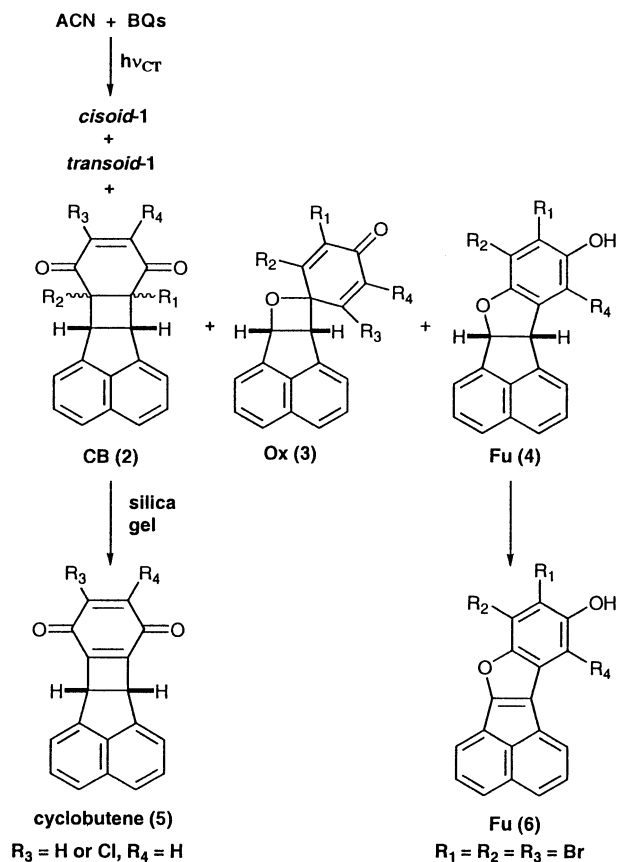
Features of reaction products

Table 2 collects the reaction products from various BQs with ACN by *the direct* and *the CT mode* excitation. For a couple of

|| Molar extinction coefficients (ϵ /M⁻¹ cm⁻¹) of ACN and BQs at 436 nm in DCE are as follows: ACN, 39; TMBQ, 38; 2,5-DMBQ, 30; BQ, 22; 2-CBQ, 24; 2-BBQ, 27; 2,5-DCBQ, 26; 2,6-DCBQ, 25; TFBQ, 24; TCBQ, 37; TBBQ, 52; DDQ, 320. It should be emphasized that at the concentration of ACN and BQs in this study, light absorbed by the CT complex is negligible compared to that of ACN and BQs due to the small K_{eq} values.

a BQ and ACN, when reaction took place from both *the direct mode* with $\lambda_{exc} > 420$ nm and *the CT mode* with $\lambda_{exc} > 500$ nm, the couple afforded essentially the same kinds of reaction products, though the distribution among them varied somewhat with the irradiation mode. In Table 2, the yields of the products represent those actually isolated by chromatography, and identified by means of spectral (EI-MS, ¹H- and ¹³C-NMR) properties and elemental analysis. (For details, see Experimental section.)

The reaction products can be classified in two categories: the dimers of ACN (*cisoid*- and *transoid*-**1**) produced always when reaction took place and the 1 : 1-adducts between ACN and BQs (Scheme 4). The latter are further divided into two groups: cyclobutanes (CB, **2**) arising from reaction of the C=C double bond of BQs;^{11,12} oxetanes (Ox, **3**) (the Paterno–Büchi reaction),^{13,14} and furans (Fu, **4**) arising from the C=O double bond of BQs. Features of formation of these products can be summarized in the following way.



Scheme 4

(1) **Product distribution from the two modes of excitation.** When the *CT* mode gave reaction products, both excitation modes led to similar product distribution; however, the *CT* mode gave a somewhat higher *cisoid/transoid* ratio of **1** than the *direct* mode. The combined yields of the 1 : 1-adducts were not much different between the two excitation modes, for example, 45, 54 and 87% by the *CT* mode, and 53, 54, and 61% by the *direct* mode for 2-CBQ, 2,5-dichloro-1,4-benzoquinone (2,5-DCBQ), and TBBQ, respectively.

(2) **Production of the 1 : 1-adducts (2, 3, 4) compared to the dimers of ACN (1).** The yields of the 1 : 1-adducts varied widely among BQs. The ratio of the 1 : 1-adducts (**2 + 3 + 4**) to the dimers (**1**) varied from 13.5 for 2,5-DCBQ to 1.52 for 2-bromo-1,4-benzoquinone (2-BBQ) for the *CT* mode, and from 8.1 for TCBQ to approaching zero for DDQ for the *direct* mode.

(3) **Distribution among the 1 : 1-adducts.** Distribution of **2**, **3** and **4** among the 1 : 1-adducts very much depended on the substitution of BQs. Many BQs afforded CB **2** or its derivatives, cyclobutenes (**5**), particularly under the *direct* mode, except 2,5-DMBQ, BQ, TFBQ, and DDQ. On the other hand, Ox **3** was formed only from 2,5-DMBQ, 2-CBQ, 2,5-DCBQ, TFBQ, TCBQ (as derivatives from Ox) and, particularly, from bromanil (TBBQ) in a high yield. Production of Fu **4** was limited from BQ, 2-CBQ, 2-BBQ and TBBQ.

(4) **Regio- and stereoselectivity of the 1 : 1-adducts.** As to formation of CB, *cisoid-2* was exclusively or more favorably produced than *transoid-2*. Thus, TMBQ gave a *cisoid* isomer of CB (**2a**) as yellow prisms in a very good yield under the *direct* mode. Two protons arising from the acenaphthene group of this CB were determined in *cisoid* alignment with the two methyl groups of the dihydrobenzoquinone moiety by X-ray crystallography of a single crystal as depicted for the ORTEP diagram

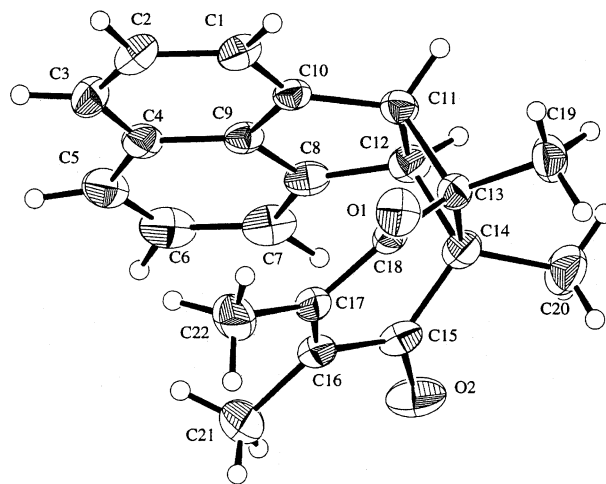


Fig. 1 ORTEP drawing of compound **2a**.

in Fig. 1 and summarized in Table 3. Likewise, 2,6-DCBQ, 2-BBQ and TBBQ afforded only *cisoid-2*, though in relatively low yield, and larger amounts of derived cyclobutene **5**. Production of cyclobutene **5** is undoubtedly due to facile thermal elimination of hydrogen halide from CB **2** (**2d**, **2e**, **2f**, **2g**) especially on silica gel during the chromatographic isolation (Scheme 4). Moreover, from 2-CBQ and 2,5-DCBQ only **5** but none of CB **2** was isolated. Among BQs examined, only TCBQ gave a mixture of *cisoid-* and *transoid-2i* in a ratio of 6 ~ 7 (Table 2).

As to Ox **3**, 2-CBQ afforded solely **3d** among four possible isomers, and 2,5-DMBQ and 2,5-DCBQ yielded **3b** and **3f**, respectively, among two. The structure of **3f** was successfully established by X-ray crystallography of a single crystal (Fig. 2 and Table 3).

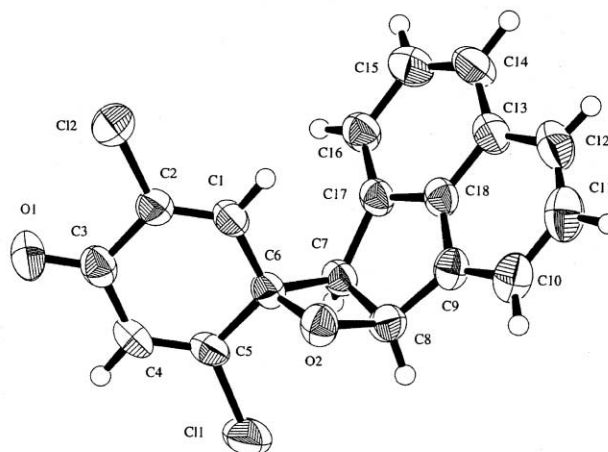


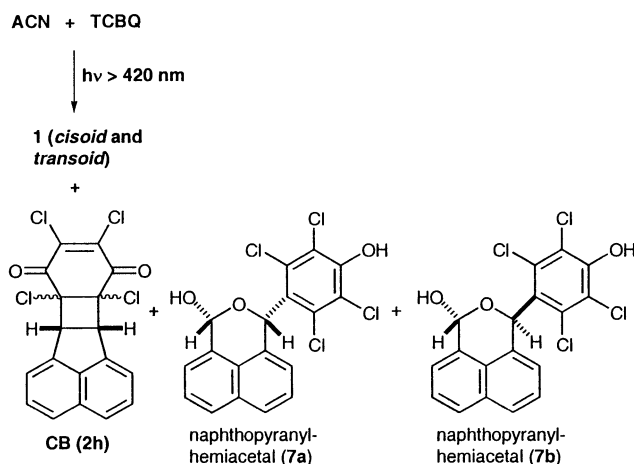
Fig. 2 ORTEP drawing of compound **3f**.

Regarding Fu **4**, 2-CBQ and 2-BBQ regioselectively afforded only one isomeric Fu (**4d** and **4e**) among the four possible isomers. TBBQ yielded Fu **4j** in a relatively high yield by way of elimination of a bromine atom (Scheme 4). A part of **4j** readily underwent thermal dehydrogenation to afford Fu **6**, which was contaminated with **4j**.

(5) **Unique reactivity of TCBQ.** A dramatic feature was noted for the case of TCBQ. As has preliminarily been reported,¹⁵ irradiation of TCBQ and ACN by the *direct* mode led to two isomeric naphthopyranylhemiacetals (**7a** and **7b**) in excellent yields together with **1** and two isomeric CB (**2i**) (Scheme 5, Table 2). Though many efforts have been devoted to investigation of the photochemical behavior of TCBQ,^{14c,16,17-28}

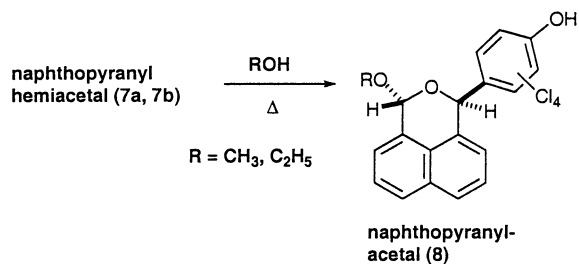
Table 3 Crystal data for compounds **2a**, **3f** and **8a**

| | 2a | 3f | 8a |
|--|---|--|--|
| Empirical formula | C ₂₂ H ₂₀ O ₂ | C ₁₈ H ₁₀ Cl ₂ O ₂ | C ₂₀ H ₁₃ Cl ₆ O ₃ |
| Color, habit | Pale yellow, Prism | Pale yellow, Prism | Colorless, Prism |
| Dimensions/mm | 0.30 × 0.40 × 0.30 | 0.40 × 0.50 × 0.10 | 0.20 × 0.20 × 0.20 |
| Crystal system | Monoclinic | Triclinic | Triclinic |
| Lattice parameters | <i>a</i> = 8.408 (1) Å <i>b</i> = 22.146 (3) Å <i>c</i> = 9.527 (2) Å <i>V</i> = 1645.5 (2) Å ³ <i>β</i> = 111.94 (2)° | <i>a</i> = 9.180 (3) Å <i>b</i> = 10.753 (2) Å <i>c</i> = 8.341 (1) Å <i>V</i> = 736.3 (3) Å ³ <i>a</i> = 103.45 (1)° <i>β</i> = 99.61 (2)° <i>γ</i> = 67.35 (2)° | <i>a</i> = 10.789 (2) Å <i>b</i> = 11.964 (2) Å <i>c</i> = 8.388 (1) Å <i>V</i> = 1046.7 (3) Å ³ <i>a</i> = 93.52 (2)° <i>β</i> = 103.84 (1)° <i>γ</i> = 85.22 (2)° |
| Space group | <i>P</i> 2 ₁ / <i>n</i> (#14) | <i>P</i> 1̄ (#2) | <i>P</i> 1̄ (#2) |
| <i>Z</i> value | 4 | 2 | 4 |
| <i>D</i> _{calc} /g cm ⁻³ | 1.277 | 1.485 | 3.262 |
| <i>μ</i> (Cu-Kα)/cm ⁻¹ | 6.33 | 39.97 | 153.49 |
| No. of reflections measured | 3172 | 2603 | 3893 |
| No. of unique reflections | 3067 | 2454 | 3683 |
| <i>R</i> _{int} | 0.019 | 0.48 | 0.079 |
| Reflection/parameter ratio | 10.93 | 10.23 | 10.49 |
| <i>R</i> | 0.081 | 0.065 | 0.063 |
| <i>R</i> _w | 0.200 | 0.130 | 0.099 |
| Goodness of fit indicator | 1.83 | 1.41 | 1.44 |



Scheme 5

no report has been found of the formation of pyran derivatives. When **7a** or **7b** was independently treated with aqueous acetonitrile, both of them anomerized to give a mixture of **7a** and **7b** with an equilibrium ratio of 2.8. This interconversion was accelerated in the presence of 10⁻³ M of hydrochloric acid. Moreover, both **7a** and **7b** were converted into a naphthopyranyl-acetal (**8**) on treatment with primary alcohols such as methanol and ethanol but not with *tert*-butyl alcohol (Scheme 6). The structure of **8a** (acetal from methanol) was established



Scheme 6

by X-ray crystallography of a single crystal composed of **8a** and dichloromethane as a crystallization solvent in a ratio of 1 : 1 (Fig. 3 and Table 3).

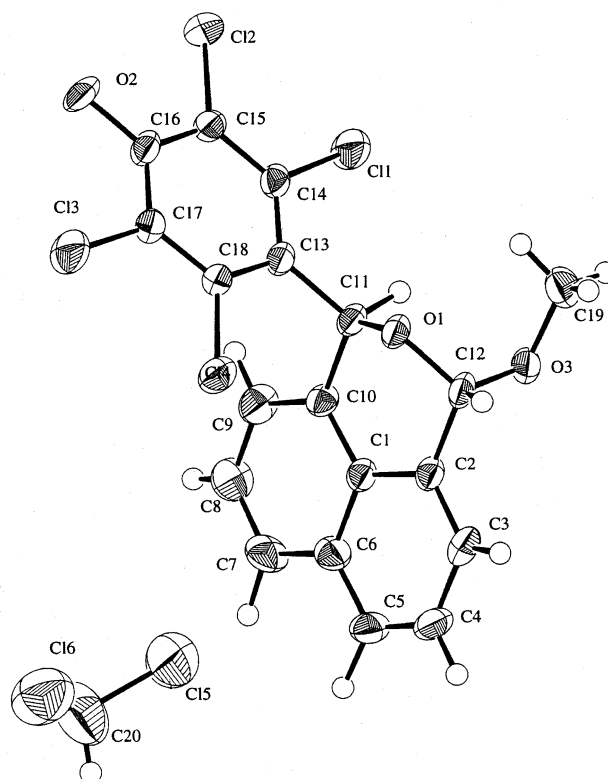
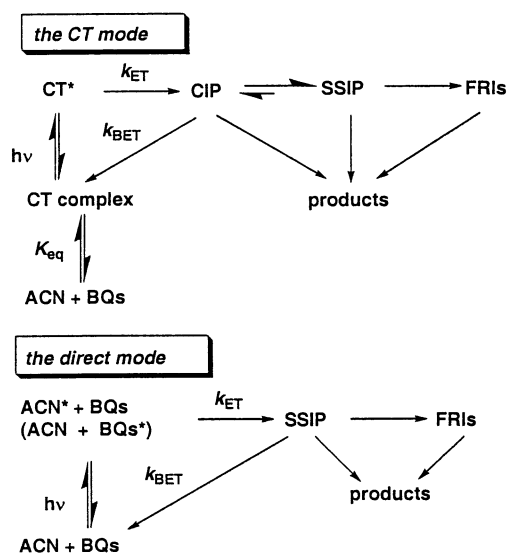


Fig. 3 ORTEP drawing of compound **8a**.

General mechanism of the reactions

In solution, the *CT mode* excitation will give the excited state of the CT complex, which will be rapidly converted into a CIP of ACN⁺ and BQ⁻; on the other hand, the *direct mode* excitation will generate excited states of either ACN or BQs which will undergo electron transfer with the encountered counterpart to afford an SSIP of ACN⁺ and BQ⁻ (Scheme 7). The CIP resulting from the *CT mode* will either undergo reaction inside the pair or convert to the SSIP, competing with deactivation by BET to the ground state. The SSIP will further dissociate to FRIs, particularly in the triplet pair, or undergo reactions in the pair competing with BET. The diffused FRIs will undergo reactions with suitable species.



Scheme 7

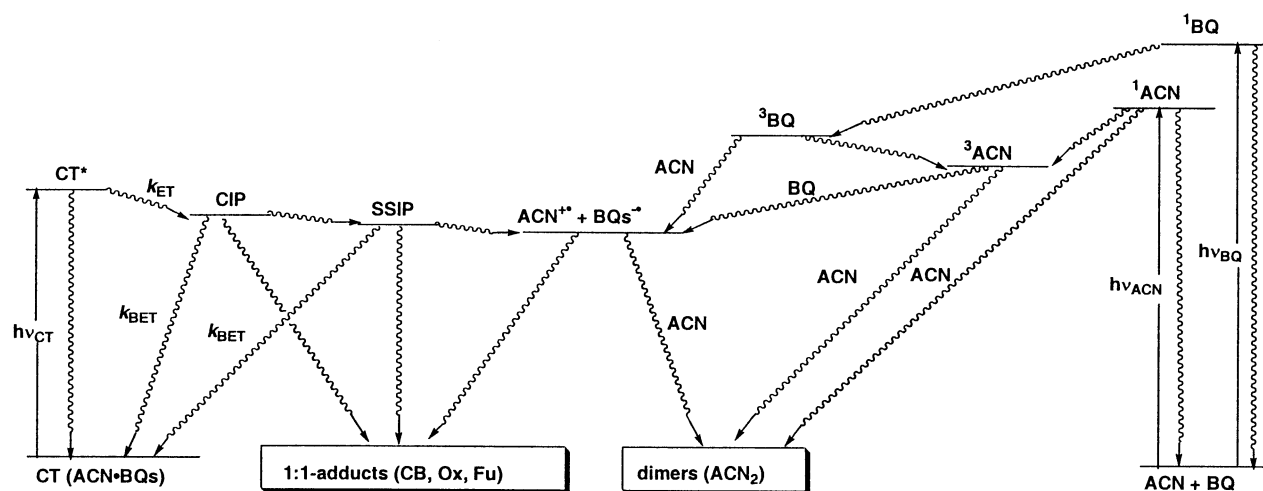
Regarding the energetics of electron transfer, the singlet excited state ACN (257 kJ mol^{-1})²⁹ lies higher in energy than all the radical ion pairs examined, CIP or SSIP, (expressed as $-\Delta G_{BET}$ in Table 1) ranging from around 100 to 200 kJ mol^{-1} ; the triplet ACN (196 kJ mol^{-1})³⁰ is also higher in energy than the radical ion pairs examined except BQ, and especially TMBQ and 2,5-DMBQ. When BQs are excited, the initially produced singlet excited states will efficiently undergo intersystem crossing to the triplet states, which seem to be higher in energy than the corresponding radical ion pairs except TMBQ and 2,5-DMBQ. Moreover, most triplet BQs seem to be higher in energy than the ACN triplet state. Accordingly, the triplet state of BQs will undergo energy transfer to ACN to give its triplet state competing with other processes. Therefore, in the *direct mode*, electron transfer to afford SSIP can take place in an exoergonic way from the ACN singlet excited state to all BQs, from the ACN triplet state to BQs except BQ, 2,5-TMBQ and TMBQ, and also from BQs triplet to ACN except TMBQ and 2,5-TMBQ, competing with triplet energy transfer to ACN. Moreover, the energy of the excited state of the CT complexes estimated from the edge (λ with ϵ of $2 \text{ cm}^{-1} \text{ M}^{-1}$) of the CT absorption spectra is higher than the corresponding radical ion pair. Accordingly, in the *CT mode*, the CT excited state will readily undergo charge separation to give a CIP. Formation of the same products with nearly the same distribution from a pair of ACN with one of the BQs by either the *CT* or the *direct mode* excitation means that the initially produced CIP or SSIP leads

to the same distribution of the final products. The general mechanisms for the product formation can be depicted as Scheme 8.

Formation of ACN dimers

As Table 2 shows, *cisoid*- and *transoid*-**1** were always formed when reaction took place, though the yields remained relatively low. Among these isomers, *cisoid*-**1** was produced more preferably than *transoid*-**1** with the *cisoid/transoid* ratio of 2.5 ~ 5.8 from the *CT mode* and 2.2 ~ 4.0 from the *direct mode* (except TMBQ and 2,5-DMBQ). These values are in accord with the results (*ca.* 5) previously observed for the ACN–TCNE couple by the *direct mode* under the same concentration as the present study.¹ Production of **1** certainly proceeds outside of the initially formed RIP, because any reactive species of ACN has to encounter the ground state of ACN out of the pair or, at least, at the wall of the solvent cage. The ratio of the *cisoid* and the *transoid* of resulting **1** provides clues for revealing the reactive species of the dimerization. As we have previously shown for the photoinduced electron transfer of the ACN–TCNE system,¹ generation of $ACN^{+•}$ by way of electron transfer from the excited ACN to TCNE and its subsequent addition to the ground state ACN leads to **1** in a high ratio of the *cisoid/transoid*. However, in the absence of electron acceptor, addition of excited states of ACN to the ground state ACN gives **1** in a lower ratio of *cisoid/transoid* (0.65) with a contribution of 31% from the singlet state, 1ACN , and 69% from the triplet state, 3ACN , at $[ACN] = 2.0 \times 10^{-2} \text{ M}$ in DCE.³¹ Therefore, a higher *cisoid/transoid* ratio of **1** is definitive evidence for participation of $ACN^{+•}$ as an intermediate; in contrast, a lower ratio reflects some contribution from the addition of the 3ACN or the 1ACN to the ground state ACN.

Therefore, the observed *cisoid/transoid* ratio of **1** resulting from both the *CT* and the *direct mode* excitation certainly indicates the participation of $ACN^{+•}$ in production of **1**. Thus, $ACN^{+•}$ resulting from the electron transfer undergoes electrophilic addition to the ground state ACN to give the dimeric radical cation of ACN, $ACN_2^{+•}$, finally leading to **1** in a higher *cisoid/transoid* ratio. However, the observed slight decrease of the ratios from the *CT mode* to the *direct mode* (for example, from 5.8 to 2.8, 4.4 to 3.1, and 2.6 to 2.2 for 2,5-DCBQ, 2,6-DCBQ, and TBBQ, respectively (Table 2)) shows minor but meaningful contribution of the 3ACN or 1ACN especially in the *direct mode*. In the *direct mode*, both ACN and BQs are excited, and both the resulting excited states will undergo electron transfer with the encountered counterpart molecules in the ground state to give $ACN^{+•}$ and $BQ^{+•}$ and, concurrently, the excited singlet and/or triplet ACN will add to the ground state ACN.



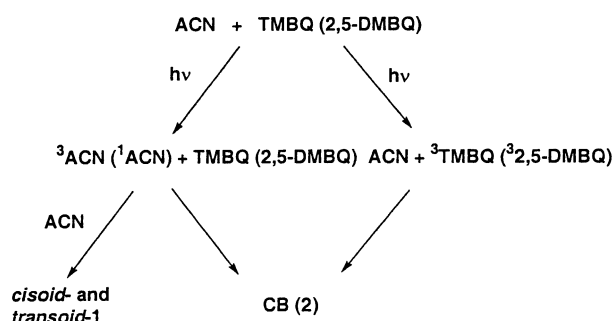
Scheme 8

Table 4 Effect of concentration of ACN and TBBQ on product distribution upon excitation by *the CT mode* in 1,2-dichloroethane^a

| [ACN]/M | [TBBQ]/M | Conversion (%) ^b | Yield (%) ^c | | | | 1/1 : 1-adducts |
|---------|----------|-----------------------------|------------------------------|--------|--------|--------|-----------------|
| | | | 1 (<i>cisoid/transoid</i>) | CB (2) | Ox (3) | Fu (4) | |
| 0.02 | 0.02 | 91 | 8 (2.3) | 8 | 64 | 12 | 0.095 |
| 0.04 | 0.02 | 85 | 16 (2.0) | 7 | 44 | 8 | 0.27 |
| 0.10 | 0.02 | 82 | 24 (2.0) | 5 | 35 | 5 | 0.53 |
| 0.20 | 0.02 | 85 | 42 (1.9) | 3 | 28 | 5 | 1.17 |
| 0.40 | 0.02 | 92 | 52 (2.4) | 1 | 25 | 4 | 1.73 |
| 0.60 | 0.02 | 80 | 56 (2.0) | 1 | 25 | 3 | 1.93 |
| 1.00 | 0.02 | 83 | 58 (1.9) | Trace | 25 | 2 | 2.14 |
| 2.00 | 0.02 | 92 | 57 (2.5) | Trace | 24 | 2 | 2.19 |
| 0.02 | 0.03 | 78 | 8 (2.1) | 6 | 59 | 15 | 0.10 |
| 0.02 | 0.04 | 84 | 10 (2.5) | 6 | 63 | 12 | 0.12 |

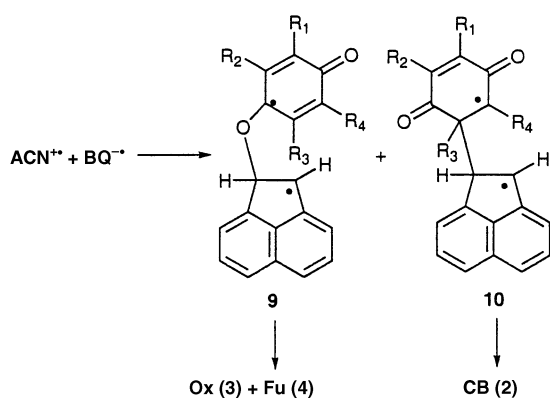
^a Exposure of light of wavelength longer than 500 nm. ^b Converted ACN after 70 hours of irradiation. ^c Yields based on ACN consumed.

The observed *cisoid/transoid* ratio of 0.70 for TMBQ and 2,5-DMBQ in *the direct mode*, which is much lower than those for the other BQs, is quite close to that of 0.65 in the absence of an electron acceptor at [ACN] = 2.0×10^{-2} M in DCE.³¹ This value means that **1** does not result from photoinduced electron transfer from TMBQ (or 2,5-TMBQ) to ACN as mentioned before from energetic viewpoints, but is produced from addition of excited states of ACN to the ground state ACN (Scheme 9).



Formation of the 1 : 1-adducts

The 1 : 1-adducts can be produced in the cage reaction inside RIP (CIP or SSIP) and by coupling between FRIs escaped from the pairs (Scheme 10). When a C–O bond is initially formed



between the alkenic C=C bond of ACN^{•+} and the carbonyl C=O bond of BQ^{•-}, biradical **9** is necessarily formed as a common intermediate for Ox **3** and Fu **4**. On the other hand, initial formation of a C–C bond between the alkenic C=C bond of ACN^{•+} and BQ^{•-} gives biradical **10** leading to CB **2**.

The effect of concentration of either ACN or TBBQ in *the CT mode* excitation proceeding in a nearly stoichiometric way

can give an insight into this task. As shown in Table 4, the yield of the dimers **1** increased with increase of [ACN] at the expense of the 1 : 1-adducts (especially Ox **3**) under constant [TBBQ] of 0.02 M. Thus, on varying [ACN] from 0.02 to 2.0 M in DCE, the yield of **1** jumped seven-fold from 8 to 57%, whereas the combined yield of **2**, **3**, and **4** fell from 84 to 26%. However, at high [ACN] the ratio of 1/1 : 1-adducts approached a plateau value of 2.2, which indicates that a part of the 1 : 1-adducts was formed irrespective of [ACN].

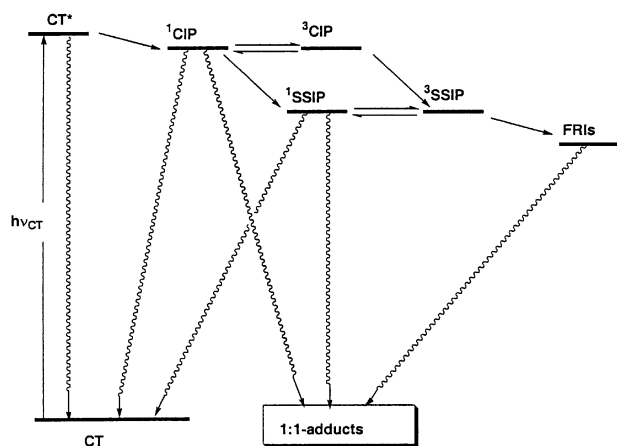
In contrast, variation of [TBBQ] was not significant for product distribution, though the range of the concentration was limited due to low solubility of TBBQ in DCE.

The above increase of **1** at the expense of the 1 : 1-adducts, especially Ox **3** (65%), with increase of [ACN] in the range of 100 fold at a constant [TBBQ] indicates participation of common reactive species such as free ACN^{•+} outside of an RIP for formation of **1** and, at least, suppressed formation of the 1 : 1-adducts. However, production of still medium amounts of Ox **3** (25%) and other 1 : 1-adducts at very high [ACN] shows a contribution of the cage reaction inside the RIP for formation of these parts of the adducts. Thus, the 1 : 1-adducts arising from the ACN–TBBQ complex are produced from coupling reactions between ACN^{•+} and TBBQ^{•-} both inside and outside of the RIP, estimated as roughly 32 and 68%, respectively. Formation of the essentially constant *cisoid/transoid* ratio (1.9 ~ 2.5) of **1** with 100 fold variation of [ACN] supports the mechanism where ACN^{•+} generated in an RIP by *the CT mode* excitation has to escape from the cage to encounter the ground state ACN to produce **1** irrespective of [ACN] employed.

Therefore, it is not very unreasonable to extend the above mechanism borne out of the ACN–TBBQ couple to that for couples of ACN and various BQs. Thus, the adducts might generally be produced both inside and outside of the solvent cage of the RIP resulting from *the CT* and *the direct mode* of excitation for various BQs because of formation of essentially the same distribution of products from both modes of excitation. Furthermore, more or less regio- and stereo-selective formation of the adducts shows that interaction between the radical ions, ACN^{•+}, and BQ^{•-}, takes place in selective ways.

If we discuss this further, comparison of the results of *the CT mode* excitation of TFBQ, TCBQ and TBBQ provides us with insight into the nature of the RIP participating in reactions. For these three BQs, electron transfer in the excited state of the CT complex to give an RIP can be estimated to proceed with sufficient decrease of free energies, $\Delta G_{ET} = -50 \sim -40$ kJ mol⁻¹, and the resulting RIP are 160 ~ 150 kJ mol⁻¹ higher in energy over the ground state. Therefore, these three BQs are supposed to behave energetically in a similar way. However, on *the CT mode* excitation, only ACN–TBBQ afforded products in contrast to ACN–TFBQ and ACN–TCBQ which gave no products at all.

Among these three BQs, TBBQ will exhibit a most remarkable heavy atom effect due to the presence of four bromine



Scheme 11

atoms to enhance intersystem crossing of the initially produced singlet CIP to the triplet pair (Scheme 11). The triplet CIP might convert to the triplet SSIP more facilely in order to reduce the interaction between the radical ions than the conversion of the singlet CIP to the singlet SSIP. The resulting triplet SSIP will undergo either diffusion to afford FRIs or conversion to the singlet SSIP, finally giving rise to net products.

On the other hand, in ACN–TFBQ and ACN–TCBQ, failure of formation of any products from *the CT mode* excitation suggests that the singlet CIP resulting from these complexes quickly undergoes BET preceding the conversion to the triplet CIP and subsequently to the triplet SSIP.

The above results of excitation of the CT complex of TBBQ are in contrast to the hitherto reported behavior of triplet SSIP. Thus, in many electron transfer processes between triplet states and counterpart molecules, the presence of heavy atoms was shown to reduce the quantum yield of the reactions.^{32–35} For example, on irradiation of brominated or iodinated xanthenes dyes such as Eosin Y, Erythrosine and their derivatives in the presence of methyl viologen as an electron acceptor and triethanolamine as a sacrificial electron donor in aqueous organic solutions, an increase in heavy atoms lowered the quantum yield for reduction of methyl viologen. Thus, the larger the sum of the spin-orbit coupling constants of heavy atoms in the dye molecules, the lower the quantum yield of the reaction.³⁵ In these reactions, the observed effect of heavy atoms was attributed to enhancement of deactivation of the triplet SSIP to the ground state.

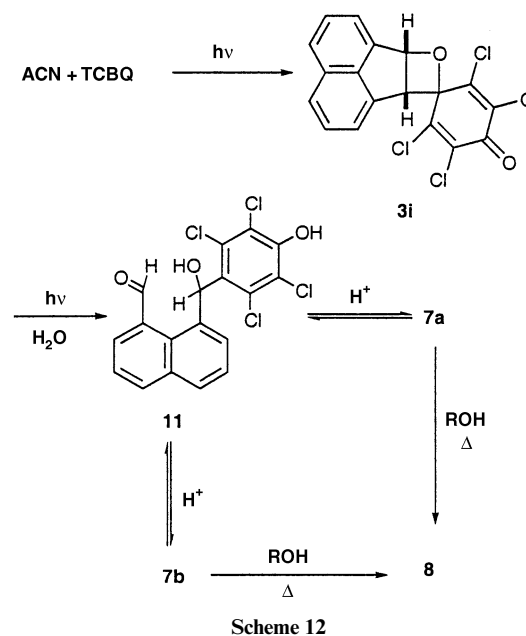
Accordingly, in the present CT mode reaction, the role of heavy atoms in enhancing the quantum yield of the reactions seems to rather accelerate the intersystem crossing of the singlet CIP, which otherwise quickly undergoes BET, to triplet CIP and subsequently triplet SSIP. Therefore, the heavy atoms show apparently reversal effects on formation of final products depending on intersystem crossing of either singlet CIP or triplet SSIP; thus, enhancement of product formation in crossing from the singlet CIP to the triplet CIP and further to triplet SSIP, but retardation of that in crossing from the triplet SSIP to the ground state.

As described before, TMBQ and 2,5-TMBQ do not undergo photoinduced electron transfer with ACN. Therefore, the formation of the 1 : 1-adduct from TMBQ and 2,5-DMBQ can be attributed to either addition of the excited states of ACN to TMBQ (2,5-DMBQ) or addition of the triplet state of TMBQ (2,5-DMBQ) to ACN, as depicted in Scheme 9. Moreover, preferential formation of the CB **2a** from TMBQ without forming other 1 : 1-adducts (Ox **3** and Fu **4**) is seemingly in accord with the $\pi\pi^*$ nature of the ³TMBQ.⁸ Stereoselective formation of *cisoid-2a* suggests that ACN and TMBQ in the excited state interact in a geometry such as an exciplex. In a similar vein,

preferential formation of Ox **3b** leads to the conclusion that the character of the excited state of 2,5-DMBQ is $n\pi^*$.

Regarding production of the naphthopyranylhemiacetals **7a** and **7b** from ACN–TCBQ under *the direct mode* excitation¹⁵

It seems quite abnormal that the naphthopyranylhemiacetals **7a** and **7b** were exceptionally produced in the ACN–TCBQ system by *the direct mode*. The mechanism for formation of **7a** and **7b** is not entirely clear at present. It is reasonably certain that the initial step of the reaction is photoinduced electron transfer between ACN and TCBQ to give an SSIP, which can be successively converted to Ox **3i** followed by subsequent photochemical hydration by eventually present water leading to 8-arylhdroxymethyl-1-naphthylaldehyde (**11**) as depicted in Scheme 12. The absence of **7** in the case of TFBQ and TBBQ



Scheme 12

may be therefore attributed to the stability of Ox **3** from these BQs towards hydration.

Quantum yields for the reactions

To investigate the effect of varying electron-accepting ability of BQs on the reactivity, quantum yields for the reactions by *the CT mode*, $\Phi_{546.1}$, and those by *the direct mode*, $\Phi_{435.8}$, were determined under irradiation of 546.1 and 435.8 nm monochromatic light, respectively. The extent of reaction was monitored by GC for unconverted ACN. The results are listed in Table 5.

Effect of $-\Delta G_{\text{BET}}$ on the reactivity

In a preliminary report on excitation of CT complexes of ACN with various acceptors including nitriles, acid anhydrides and limited kinds of BQs, we have shown a clear trend that *the CT mode* excitation of the CT complexes with large $-\Delta G_{\text{BET}}$ gives net products; however, with lowering of $-\Delta G_{\text{BET}}$, reactivity of the complexes tends to decrease, finally to entirely zero when $-\Delta G_{\text{BET}}$ is lower than *ca.* 160 kJ mol⁻¹.² The present results employing CT complexes of ACN with eleven kinds of BQs of widely varying reduction potentials further confirm the above concept. Thus, with lowering of $-\Delta G_{\text{BET}}$, quantum yields *giving actual reaction products*, $\Phi_{546.1}$, tend to decrease, finally to zero below a threshold value of $-\Delta G_{\text{BET}}$ due to acceleration of BET, except some of the CT complexes, particularly ACN–TBBQ affected by the presence of heavy atoms. This conforms with Mataga *et al.*'s transient absorption spectroscopy results on

Table 5 Quantum yields ($\Phi_{435.8}$ and $\Phi_{546.1}$) for photochemical reactions of ACN with various electron acceptors on irradiation with 435.8 and 546.1 nm monochromatic light in 1,2-dichloroethane^a

| Acceptor ^b | $\Phi_{435.8}$ ^c | $\Phi_{546.1}$ ^c |
|-----------------------|-----------------------------|-----------------------------|
| TMBQ | 0.088 (0.015) | — |
| 2,5-DMBQ | 0.067(0.010) | — |
| BQ | 0.048 (0.010) | 0.0026 (0.002) |
| 2-CBQ | 0.083 (0.017) | 0.014 (0.002) |
| 2-BBQ | 0.100 (0.012) | 0.010 (0.002) |
| 2,5-DCBQ | 0.089 (0.017) | 0.0090 (0.002) |
| 2,6-DCBQ | 0.095 (0.015) | 0.013 (0.002) |
| TFBQ | 0.101 (0.013) | 0 |
| TCBQ | 0.108 (0.013) | 0 |
| TBBQ | 0.112 (0.020) | 0.018 (0.003) |
| DDQ | 0.182 (0.028) | 0 |
| DDQ | 0.092 (0.014) ^d | 0 |
| DDQ | 0.058 (0.011) ^e | 0 |
| ^f | 0.032 (0.006) | — |

^a [ACN] = 2.0×10^{-2} M, [BQs] = 2.0×10^{-2} M in 1,2-dichloroethane.

^b Acceptors are listed in a sequence of increasing $E_{1/2}^{\text{Red}}$. ^c Standard deviations in parentheses. ^d [ACN] = 2.0×10^{-2} M, [DDQ] = 5.0×10^{-3} M. ^e [ACN] = 2.0×10^{-2} M, [DDQ] = 1.0×10^{-3} M. ^f Direct excitation of ACN without acceptor.

excitation of CT complexes of aromatic hydrocarbons with acid anhydrides and nitriles, though different couples of compounds from ours, that the rate constants for the decay of the resulting CIP are linearly increased with decrease of $-\Delta G_{\text{BET}}$.⁴

The $\Phi_{546.1}$ is nevertheless not more than 0.02, which is 5.9 ~ 18.5 times lower in magnitude than the $\Phi_{435.8}$ for each BQ (Table 5). This phenomenon indicates that a CIP undergoes BET more rapidly than dissociation even for CIPs with large $-\Delta G_{\text{BET}}$. Significantly higher values for $\Phi_{435.8}$ than for $\Phi_{546.1}$ can therefore be attributed to the absence of a CIP in the course of the reaction by the *direct mode*.

The $\Phi_{435.8}$ values collected in Table 5 are very complex without a manifest trend with $-\Delta G_{\text{BET}}$. This may reflect the contribution of a plural reaction path to the $\Phi_{435.8}$; namely, electron transfer from excited ACN or BQs to the ground state counterpart to give a triplet SSIP and addition of excited ACN (singlet or triplet) to the ground state ACN to give the dimers **1**.

The present results with widely varying $E_{1/2}^{\text{Red}}$ of BQs are in keeping with results of previous work carried out for a few kinds of BQs; for example, TCBQ and 2,6-DCBQ underwent photoinduced electron transfer with their counterparts more efficiently on direct excitation of BQs proceeding *via* triplet SSIPs than on selective excitation of their CT complexes proceeding *via* CIPs.^{23,36}

An abnormally high $\Phi_{435.8}$ for DDQ may be attributed to a destructive reaction from the excited DDQ without affording products which is to be identified.

Conclusions

We have carried out photochemical reactions between ACN and eleven kinds of BQs of varying reduction potential by aiming at isolation and identification of final products and measurement of quantum yields of the reactions. In solution, almost all BQs except TMBQ and 2,5-DMBQ formed ground state CT complexes with ACN. Excitation by both the *CT* and the *direct mode* produced the dimers of ACN (**1**) and the 1 : 1-adducts (**2**, **3**, and **4**) except for the cases of TFBQ, TCBQ and DDQ which were inert by the *CT mode*. Exceptional products were the naphthopyranylehemiacetals (**7a** and **7b**) between ACN and TCBQ by the *direct mode*, which were anomerized to each other like sugars and were converted into an identical naphthopyranylehemiacetal (**8**) by alcoholysis. Distribution among these products depended on the substituents on the BQ ring. However, both modes resulted in essentially identical distribution of products when the *CT mode* was reactive. As depicted in

Scheme 8, excitation of the CT complexes by the *CT mode* will induce electron transfer from ACN to BQs to generate a CIP, which undergoes facile BET to the ground state competing with the foregoing dissociation to FRIs *via* an SSIP. On the other hand, the *direct mode* excitation will generate excited states of either ACN or BQs which will undergo electron transfer with the encountered counterpart to afford an SSIP, which more readily dissociates to FRIs due to slower BET than a CIP.

In both modes ACN⁺⁺ dissociated from the SSIP will add to the ground state ACN to produce the dimers **1**. A preference for *cisoid-1* over *transoid-1* except in the case of TMBQ and 2,5-DMBQ can be used to diagnose the participation of ACN⁺⁺ in the dimer formation which gives a high ratio of *cisoid-1*. The somewhat low value of the *cisoid/transoid* ratio in the *direct mode* reflects participation of another path for dimerization of ACN by direct attack of excited ACN on the ground state ACN.

The 1 : 1-adducts can be produced from both cage reaction in the RIP (CIP and SSIP) and reaction between FRIs (ACN⁺⁺ and BQ^{-•}) because, for ACN–TBBQ, they were still produced under the condition of as high as 100 times in magnitude of [ACN] to [TBBQ].

For excitation of each couple of ACN and BQs, the $\Phi_{546.1}$ was lower than $\Phi_{435.8}$, when the CT complex was reactive. It is noteworthy that, in the *CT mode*, the $\Phi_{546.1}$ tended to increase with increase of $-\Delta G_{\text{BET}}$ due to retardation of BET from the CIP.

In conclusion, there is no doubt that $-\Delta G_{\text{BET}}$ is at least one of the essential factors to control reactivity from the excited CT complexes of ACN with BQs and the resulting CIP leading to final products in solution. We feel, however, that a contribution from other factors such as intersystem crossing from the singlet RIP (CIP or SSIP) to the triplet one to retard BET and to accelerate dissociation to FRIs may also determine reactivity from excited CT complexes.

Experimental

General

Melting points were obtained on a Yazawa melting point apparatus (type BY-10) without correction. ¹H-NMR spectra were determined with a Varian UNITY 400 spectrometer or a JEOL JNM-AL400 spectrometer in various solvents, with tetramethylsilane as an internal reference. UV spectra were obtained on a Hitachi UV-VIS 340 spectrophotometer. Low-resolution electron ionization mass spectra (EI-MS) were taken on a JEOL JMS-DX 300 or JMS-SX 102A. GC was taken on a Shimadzu GC 14-A equipped with a Chromatopac C-R5A. Flash column chromatography was performed on silica gel (Merck Art 9385 Kieselgel 60). Thin layer chromatography (TLC) was performed on silica gel (Merck Art 11696 TLC-Kieselgel 60 HF). Microanalyses were carried out in the micro-analytical laboratory of the School of Pharmaceutical Sciences, Kitasato University.

Materials and solvents

Purification of ACN has been described elsewhere.³¹ BQ (Wako) was sublimed *in vacuo* and stored in the dark. 2-CBQ (Aldrich), 2,5-DCBQ (Tokyo Kasei) and 2,6-DCBQ (Tokyo Kasei) were recrystallized from dichloromethane–hexane. 2-BBQ was prepared from bromohydroquinone according to the literature.³⁷ TCBQ (Wako) and TBBQ (Tokyo Kasei) were recrystallized from glacial acetic acid. DDQ (Tokyo Kasei) was recrystallized from benzene. TMBQ (Tokyo Kasei) was recrystallized from ethanol. 2,5-DMBQ (Tokyo Kasei) and TFBQ (Tokyo Kasei) were used as received. Potassium ferrioxalate was synthesized according to the literature.³⁸ HPLC grade DCE (Wako) and AN (Wako) as solvents for photolysis were used as supplied.

Apparatus for photolysis

As the light source, a high-pressure mercury lamp was employed with colored-glass filters. The merry-go-round apparatus for irradiation is described elsewhere.³⁹ Filtering of > 420 nm and > 500 nm light was according to the previous method.⁴⁰

CT absorption spectra of ACN with BQs and measurement of K_{eq}

A solution of 2.0×10^{-1} M of ACN in DCE was prepared in a quartz cuvette and the UV-Vis absorption spectrum was recorded. Then a stock solution (0.10 M) of BQs in DCE was added with a microsyringe and the absorption spectrum of the resultant solution was recorded. To determine the equilibrium constant of CT complexes, BQs were incrementally added so that the concentration of BQs typically ranged from 2.0×10^{-3} to 1.0×10^{-2} M, and the absorption change at an appropriate wavelength which does not overlap with that of ACN and BQs was chosen to apply to the procedure of Benesi and Hildebrand.¹⁰ Except for the case of DDQ, the λ_{max} of the CT complex is concealed among the intensive absorption of ACN and BQs in the region of 400–500 nm, so a wavelength with a large absorption gap in the presence and in the absence of BQs was chosen to determine K_{eq} as shown in Table 1.

Photochemical reaction of ACN in the presence of BQs

As a typical run, irradiation of ACN in the presence of TMBQ in DCE will be described. A solution of 304.0 mg (2.0 mmol) of ACN and 328.0 mg (2.0 mmol) of TMBQ in 100 ml of DCE was prepared in two Pyrex test tubes and purged with argon gas for 30 min and sealed. This solution was then irradiated with > 420 nm light in a merry-go round apparatus for 24 hours. After evaporation of the solvent under reduced pressure, the residual solid (642 mg) was flash-chromatographed (silica gel, eluent: hexane), which gave 18.3 mg (6.0%) of ACN, 25.2 mg (8.3%) of *cisoid-1*, and 36.2 mg (11.9%) of *transoid-1*. Gradient elution (hexane–ethyl acetate 20 : 1 then 8 : 1) gave 61.8 mg (18.8%) of TMBQ and 488.5 mg (77.3%) of *cisoid-2a* in this order. Irradiation in AN gave a similar result.

cis-cisoid-cis-6c,8,9,10a-Tetramethyl-6b,6c,10a,10b-tetrahydrobenzo[3,4]cyclobuta[1,2-a]acenaphthylene-7,10-dione (cisoid-2a). Yellow prisms, mp 201.0–202.0 °C. Anal. Calcd for $C_{22}H_{20}O_2$: C, 83.52; H, 6.37; O, 10.11. Found: C, 83.44; H, 6.51%. EI-MS: m/z 316 (M^+). ¹H-NMR (400 MHz, $CDCl_3$): δ 7.58 (d, 2H, $J = 8.1$ Hz), 7.40 (dd, 2H, $J = 8.1, 7.2$ Hz), 7.09 (d, 2H, $J = 7.2$ Hz), 4.13 (s, 2H), 1.70 (s, 6H), 1.01 (s, 6H). ¹³C-NMR (100 MHz, $CDCl_3$): δ 199.3, 145.0, 143.2, 141.7, 131.0, 128.0, 123.3, 121.7, 53.2, 52.9, 19.9, 12.4.

2',5'-Dimethyl-6b,8a-dihydrospiro[acenaphtho[1,2-b]oxete-8,1'-cyclohexa[2',5']dien]-4'-one (3b). Recrystallized from dichloromethane–hexane, pale yellow prisms which were significantly sensitive to white light, mp 104.5–108.5 (dec.) °C. Anal. Calcd for $C_{20}H_{16}O_2$: C, 83.31; H, 5.59; O, 11.10. Found: C, 83.20, H, 5.72%. EI-MS: m/z 288 (M^+). ¹H-NMR (400 MHz, $CDCl_3$): δ 7.82 (dd, 1H, $J = 7.2, 2.2$ Hz), 7.80 (d, 1H, $J = 8.3$ Hz), 7.52–7.64 (m, 3H), 7.33 (dd, 1H, $J = 3.2, 1.2$ Hz), 7.23 (d, 1H, $J = 7.2$ Hz), 6.35 (d, 1H, $J = 5.2$ Hz), 5.86 (dd, 1H, $J = 3.2, 1.2$ Hz), 4.59 (d, 1H, $J = 5.2$ Hz), 2.00 (d, 3H, $J = 1.2$ Hz), 1.65 (d, 3H, $J = 1.2$ Hz). ¹³C-NMR (100 MHz, $CDCl_3$): δ 186.4, 143.8, 143.1, 141.5, 141.0, 139.9, 135.5, 134.2, 131.8, 128.20, 128.17, 125.7, 124.3, 121.4, 121.3, 81.7, 80.9, 52.9, 16.0, 15.9.

6b,11b-Dihydroacenaphtho[1,2-b][1]benzofuran-10-ol (4c). Recrystallized from dichloromethane–hexane, dark brown cubes, mp 212.0–213.5 °C (dec.). Anal. Calcd for $C_{18}H_{12}O_2$: C, 83.06; H, 4.65; O, 12.29. Found: C, 82.92, H, 4.85%. EI-MS: m/z 260. ¹H-NMR (400 MHz, $CDCl_3$): δ 7.78 (d, 1H,

$J = 8.1$ Hz), 7.65–7.70 (m, 2H), 7.58 (dd, 2H, $J = 8.1, 7.0$ Hz), 7.49–7.54 (m, 2H), 6.98 (dd, 1H, $J = 2.8, 1.0$ Hz), 6.62 (d, 1H, $J = 8.8$ Hz), 6.61 (d, 1H, $J = 8.0$ Hz), 6.55 (dd, 1H, $J = 8.8, 2.8$ Hz), 5.35 (dd, 1H, $J = 8.0, 1.0$ Hz), 4.35 (br s, 1H). ¹³C-NMR (100 MHz, $CDCl_3$): δ 153.7, 149.8, 144.1, 141.9, 137.3, 131.6, 129.1, 128.4, 128.3, 125.6, 123.7, 121.9, 119.0, 115.3, 111.8, 110.3, 88.8, 52.4.

6b,10b-Dihydrobenzo[3,4]cyclobuta[1,2-a]acenaphthylene-7,10-dione (5a). Dark red prisms, mp > 300 °C. EI-MS: m/z 258. ¹H-NMR (400 MHz, $CDCl_3$): δ 7.71 (d, 2H, $J = 8.3$ Hz), 7.56 (d, 2H, $J = 7.5$ Hz), 7.50 (dd, 2H, $J = 8.3, 7.5$ Hz), 6.48 (s, 2H), 5.24 (s, 2H). ¹³C-NMR (100 MHz, $CDCl_3$): δ 182.1, 152.3, 138.9, 137.6, 136.4, 132.4, 127.9, 124.6, 121.8, 52.9.

2'-Chloro-6b,8a-dihydrospiro[acenaphtho[1,2-b]oxete-8,1'-cyclohexa[2',5']dien]-4'-one (3d). Colorless solid. EI-MS: m/z 294 (M^+), 296 ($M^+ + 2$). ¹H-NMR (400 MHz, $CDCl_3$): δ 7.88 (m, 1H), 7.82 (d, 1H, $J = 8.3$ Hz), 7.63 (m, 2H), 7.57 (dd, 1H, $J = 7.0, 8.0$ Hz), 7.26 (d, 1H, $J = 7.0$ Hz), 6.55 (d, 1H, $J = 5.6$ Hz), 6.50 (d, 1H, $J = 2.0$ Hz), 6.12 (d, $J = 10.0$ Hz), 5.70 (dd, 1H, $J = 10.0, 2.0$ Hz), 4.88 (d, 1H, $J = 5.6$ Hz).

9-Chloro-6b,11b-dihydroacenaphtho[1,2-b][1]benzofuran-10-ol (4d). Colorless powder, mp 182.0–183.0 °C (dec.). Anal. Calcd for $C_{18}H_{11}ClO_2$: C, 73.35; H, 3.76; Cl, 12.03; O, 10.86. Found: C, 73.22; H, 3.99; Cl, 11.89. EI-MS: m/z 294 (M^+), 296 ($M^+ + 2$). ¹H-NMR (400 MHz, $CDCl_3$): δ 7.79 (d, 1H, $J = 8.0$ Hz), 7.69 (t, 1H, $J = 6.0$ Hz), 7.68 (d, 1H, $J = 7.8$ Hz), 7.59 (dd, 1H, $J = 8.0, 7.8$ Hz), 7.52 (d, 2H, $J = 6.0$ Hz), 7.14 (s, 1H), 6.73 (s, 1H), 6.62 (d, 1H, $J = 8.0$ Hz), 5.33 (d, 1H, $J = 8.0$ Hz), 5.05–5.18 (br s, 1H). ¹³C-NMR (100 MHz, $CDCl_3$): δ 153.4, 145.6, 143.5, 141.3, 137.2, 131.5, 128.5, 128.4, 128.3, 125.7, 123.8, 122.0, 119.0, 112.5, 110.1, 110.0, 89.3, 52.2.

cis-cisoid-cis-6c-Bromo-6b,6c,10a,10b-tetrahydrobenzo[3,4]cyclobuta[1,2-a]acenaphthylene-7,10-dione (cisoid-2e). This compound was obtained as a dark brown solid being contaminated by cyclobutene **5a**. EI-MS: m/z 338 (M^+), 340 ($M^+ + 2$). ¹H-NMR (400 MHz, $CDCl_3$): δ 7.88 (d, 1H, $J = 8.4$ Hz), 7.82 (d, 1H, $J = 8.4$ Hz), 7.72 (t, 1H, $J = 8.4$ Hz), 7.64 (d, 1H, $J = 8.4$ Hz), 7.59 (dd, 1H, $J = 8.4, 7.3$ Hz), 7.46 (d, 1H, $J = 7.3$ Hz), 7.17 (d, 1H, $J = 10.5$ Hz), 7.00 (dd, 1H, $J = 10.5, 1.2$ Hz), 4.75 (dd, 1H, $J = 7.0, 1.0$ Hz), 4.32 (t, 1H, $J = 7.0$ Hz), 3.62 (dt, 1H, $J = 7.0, 1.0$ Hz).

9-Bromo-6b,11b-dihydroacenaphtho[1,2-b][1]benzofuran-10-ol (4e). Pale brown powder. EI-MS: m/z 338 (M^+), 340 ($M^+ + 2$). ¹H-NMR (400 MHz, $CDCl_3$): δ 7.72 (d, 1H, $J = 7.8$ Hz), 7.67 (t, 1H, $J = 6.3$ Hz), 7.64 (d, 1H, $J = 7.7$ Hz), 7.57 (dd, 1H, $J = 7.8, 7.7$ Hz), 7.52 (d, 2H, $J = 6.3$ Hz), 7.14 (d, 1H, $J = 0.6$ Hz), 6.86 (d, 1H, $J = 0.6$ Hz), 6.62 (d, 1H, $J = 7.9$ Hz), 5.30 (d, 1H, $J = 7.9$ Hz), 5.02–5.18 (br s, 1H). ¹³C-NMR (100 MHz, $CDCl_3$): δ 153.8, 146.6, 143.5, 141.4, 137.3, 131.7, 129.6, 128.36, 128.33, 125.7, 123.8, 122.0, 119.1, 112.8, 111.8, 109.1, 89.4, 52.2.

8-Chloro-6b,10b-dihydrobenzo[3,4]cyclobuta[1,2-a]acenaphthylene-7,10-dione (5b). Dark red powder, mp 191.0–193.5 °C (dec.). EI-MS: m/z 292 (M^+), 294 ($M^+ + 2$). ¹H-NMR (400 MHz, $CDCl_3$): δ 7.72 (d, 2H, $J = 7.8$ Hz), 7.58 (d, 1H, $J = 7.0$ Hz), 7.56 (d, 1H, $J = 7.0$ Hz), 7.51 (dd, 1H, $J = 8.0, 7.0$ Hz), 7.50 (dd, 1H, $J = 8.0, 7.0$ Hz), 6.73 (s, 1H), 5.21–5.27 (m, 2H). ¹³C-NMR (100 MHz, $CDCl_3$): δ 179.4, 173.4, 152.3, 150.8, 143.4, 136.94, 136.88, 133.3, 133.2, 132.2, 127.81, 127.85, 124.63, 124.67, 121.77, 121.81, 52.5, 52.2.

cis-cisoid-cis-6c,8-Dichloro-6b,6c,10a,10b-tetrahydrobenzo[3,4]cyclobuta[1,2-a]acenaphthylene-7,10-dione (cisoid-2g). This compound was obtained as a dark red powder being contaminated by cyclobutene **5b**. EI-MS: m/z 328 (M^+), 330 ($M^+ + 2$),

332 ($M^+ + 4$). $^1\text{H-NMR}$ (400 MHz, CDCl_3): δ 7.80 (d, 1H, $J = 8.0$ Hz), 7.73 (d, 1H, $J = 8.2$ Hz), 7.62 (t, 1H, $J = 7.0$ Hz), 7.57 (d, 1H, $J = 7.5$ Hz), 7.50 (dd, 1H, $J = 8.2, 8.0$ Hz), 7.38 (d, 1H, $J = 7.5$ Hz), 7.21 (d, 1H, $J = 1.2$ Hz), 4.75 (dd, 1H, $J = 6.8, 1.2$ Hz), 4.14 (t, 1H, $J = 6.8$ Hz), 3.47 (dt, 1H, $J = 6.8, 1.2$ Hz).

2',5'-Dichloro-6b,8a-dihydrospiro[acenaphtho[1,2-*b*]oxete-8,1'-cyclohexa[2',5']dien]-4'-one (3f). Colorless prisms, mp 132.0–133.0 °C (dec.). EI-MS: m/z 328 (M^+), 330 ($M^+ + 2$), 332 ($M^+ + 4$). $^1\text{H-NMR}$ (400 MHz, CDCl_3): δ 7.91 (dd, 1H, $J = 7.0, 2.3$ Hz), 7.86 (d, 1H, $J = 8.5$ Hz), 7.58–7.67 (m, 3H), 7.30 (d, 1H, $J = 7.0$ Hz), 6.60 (s, 1H), 6.55 (d, 1H, $J = 5.5$ Hz), 6.28 (s, 1H), 4.91 (d, 1H, $J = 5.5$ Hz). $^{13}\text{C-NMR}$ (100 MHz, CDCl_3): δ 176.1, 156.2, 142.5, 142.4, 141.6, 137.9, 131.8, 131.6, 128.3, 126.8, 126.7, 126.1, 125.0, 121.8, 121.5, 84.3, 84.2, 53.8.

2',3',5',6'-Tetrafluoro-6b,8a-dihydrospiro[acenaphtho[1,2-*b*]oxete-8,1'-cyclohexa[2',5']dien]-4'-one (3h). Recrystallized from dichloromethane–hexane, pale yellow prisms which were significantly sensitive to white light, mp 140.5–142.5 °C (dec.). Anal. Calcd for $\text{C}_{18}\text{H}_8\text{F}_4\text{O}_2$: C, 65.07; H, 2.43; F, 22.87; O, 9.63. Found: C, 65.02; H, 2.67; F, 22.65%. EI-MS: m/z 332 (M^+). $^1\text{H-NMR}$ (400 MHz, CDCl_3): δ 7.90 (dd, 1H, $J = 6.8, 2.0$ Hz), 7.85 (d, 1H, $J = 8.0$ Hz), 7.60–7.67 (m, 2H), 7.58 (dd, 1H, $J = 8.0, 7.2$ Hz), 7.36 (d, 1H, $J = 6.8$ Hz), 6.59 (d, 1H, $J = 5.2$ Hz), 5.16 (d, 1H, $J = 5.2$ Hz). $^{13}\text{C-NMR}$ (100 MHz, CDCl_3): δ 171.17 (tt, $J = 21.2, 7.6$ Hz), 153.4 (dt, $J = 96.4, 10.6$ Hz), 150.6 (dt, $J = 99.5, 10.7$ Hz), 141.9 (s), 140.1 (s), 138.7 (dt, $J = 63, 7.6$ Hz), 136.6 (s), 136.0 (dt, $J = 64.5, 6.8$ Hz), 131.8 (s), 128.5 (s), 128.4 (s), 126.6 (s), 125.5 (s), 122.2 (s), 121.1 (s), 85.3 (s), 81.6 (t, $J = 22.0$ Hz), 51.7 (s).

For data of the products from the ACN–TCBQ system (*cisoid*- and *transoid*-**2i**, **7a**, **7b**, **8a**, and **8b**), refer to our preliminary paper.¹⁵

***cis-cisoid-cis*-6c,8,9,10a-Tetrabromo-6b,6c,10a,10b-tetrahydrobenzo[3,4]cyclobuta[1,2-*a*]acenaphthylene-7,10-dione (*cisoid*-**2j**).** This compound was obtained as pale yellow prisms being contaminated by *transoid*-**1**. EI-MS: m/z 574 ($M^+ + 2$), 576 ($M^+ + 4$), 578 ($M^+ + 6$). $^1\text{H-NMR}$ (400 MHz, CDCl_3): δ 7.80 (d, 2H, $J = 8.2$ Hz), 7.62 (dd, 2H, $J = 8.2, 7.2$ Hz), 7.45 (d, 2H, $J = 7.2$ Hz), 5.10 (s, 2H).

2',3',5',6'-Tetrabromo-6b,8a-dihydrospiro[acenaphtho[1,2-*b*]oxete-8,1'-cyclohexa[2',5']dien]-4'-one (3j). Dark green prisms, mp 163.0–165.5 °C (dec.). EI-MS: m/z 574 ($M^+ + 2$), 576 ($M^+ + 4$), 578 ($M^+ + 6$). $^1\text{H-NMR}$ (400 MHz, CDCl_3): δ 7.85 (dd, 1H, $J = 7.2, 1.5$ Hz), 7.81 (d, 1H, $J = 7.8$ Hz), 7.65 (dd, 1H, $J = 7.2, 1.5$ Hz), 7.62 (t, 1H, $J = 7.2$ Hz), 7.55 (dd, $J = 7.8, 7.2$ Hz), 7.16 (d, 1H, $J = 6.6$ Hz), 4.88 (d, 1H, $J = 6.6$ Hz). $^{13}\text{C-NMR}$ (100 MHz, CDCl_3): δ 169.4, 152.1, 150.1, 143.7, 140.0, 138.3, 136.4, 131.1, 128.6, 128.3, 126.2, 125.8, 125.4, 122.4, 121.5, 90.3, 85.0, 58.7.

8,9,11-Tribromo-6b,11b-dihydroacenaphtho[1,2-*b*][1]benzofuran-10-ol (4j). Colorless powder, mp 225.0–227.0 °C (dec.). EI-MS: m/z 494 (M^+), 496 ($M^+ + 2$), 498 ($M^+ + 4$), 500 ($M^+ + 6$). $^1\text{H-NMR}$ (400 MHz, CDCl_3): δ 8.08 (d, 1H, $J = 7.5$ Hz), 7.84 (d, 1H, $J = 8.0$ Hz), 7.77 (d, 1H, $J = 7.5$ Hz), 7.75 (d, 1H, $J = 8.0$ Hz), 7.63 (dd, 1H, $J = 8.0, 7.5$ Hz), 7.53 (dd, 1H, $J = 8.0, 7.5$ Hz), 6.69 (d, 1H, $J = 7.6$ Hz), 5.61–5.67 (br s, 1H), 5.58 (d, 1H, $J = 7.6$ Hz). $^{13}\text{C-NMR}$ (100 MHz, CDCl_3): δ 152.3, 144.6, 141.9, 139.8, 137.7, 131.6, 128.9, 128.3, 128.2, 126.2, 124.5, 122.4, 122.0, 112.2, 105.8, 105.0, 89.3, 55.1.

8,9,11-Tribromoacenaphtho[1,2-*b*][1]benzofuran-10-ol (6). Yellow powder, mp 245.0–248.0 °C (dec.). EI-MS: m/z 492 (M^+), 494 ($M^+ + 2$), 496 ($M^+ + 4$), 498 ($M^+ + 6$). $^1\text{H-NMR}$ (400 MHz, CDCl_3): δ 8.36 (d, 1H, $J = 7.1$ Hz), 7.98 (d, 1H, $J = 7.1$ Hz), 7.93 (d, 1H, $J = 8.8$ Hz), 7.82 (d, 1H, $J = 8.8$ Hz), 7.64

(dd, 1H, $J = 8.8, 7.1$ Hz), 7.61 (dd, 1H, $J = 8.8, 7.1$ Hz), 6.69 (d, 1H, $J = 7.6$ Hz), 5.92–6.04 (br s, 1H). $^{13}\text{C-NMR}$ (100 MHz, $\text{DMSO-}d_6$): δ 129.39, 129.36, 128.5, 127.9, 127.7, 127.5, 127.27, 127.25, 126.0, 124.95, 124.93, 124.3, 122.4, 121.88, 121.69, 111.8, 106.9, 100.7.

Quantum yields for reactions of ACN with BQs

Monochromicity at 435.8 and 546.1 nm for measurement of quantum yields has been described elsewhere.^{1,31} A detailed procedure for the quantum yield measurements is described in our previous report employing ferrioxalate actinometry.^{1,31} Irradiation time was controlled to keep the conversion low.

X-Ray crystallographic analysis

The cell dimensions and diffraction intensities were measured on a Rigaku AFC5R diffractometer using graphite monochromatic Cu-K α radiation ($\lambda = 1.54178$ Å) and a 12 kW rotating anode generator at 23 °C. Reflections measured were collected for Lorentz and polarization factors but not for absorption. The structures were elucidated by a direct method using TEXSAN.⁴¹ At the final stage, the non-hydrogen atoms were refined anisotropically by the full-matrix least-squares refinement. A difference Fourier synthesis was calculated and the positions of all hydrogen atoms were found, and were refined isotropically. Details of the crystal data are summarized in Table 3.

Registry numbers

ACN, 208-96-8; *cisoid*-**1**, 15065-28-8; *transoid*-**1**, 14620-98-5; TMBQ, 527-17-3; 2,5-DMBQ, 137-18-8; BQ, 106-51-4; 2-CBQ, 695-99-8; 2-BBQ, 3958-82-5; 2,5-DCBQ, 615-93-0; 2,6-DCBQ, 697-91-6; TFBQ, 527-211-9; TCBQ, 118-75-2; TBBQ, 488-48-2; DDQ, 84-58-2; bromohydroquinone, 583-69-7.

Supporting information available

Crystallographic data for compounds **2b**, **3e** and **8a**. CCDC reference numbers 164736–164738.

Acknowledgements

This work was partly supported by a Kitasato University Research Grant for Young Researchers (N.H.).

References

- 1 N. Haga, H. Nakajima, H. Takayanagi and K. Tokumaru, *J. Org. Chem.*, 1998, **62**, 5372.
- 2 N. Haga, H. Takayanagi and K. Tokumaru, *Chem. Commun.*, 1998, 2093.
- 3 N. Haga, H. Nakajima, H. Takayanagi and K. Tokumaru, *Chem. Commun.*, 1997, 1171.
- 4 (a) H. Miyasaka, S. Ojima and N. Mataga, *J. Phys. Chem.*, 1989, **93**, 3380; (b) S. Ojima, H. Miyasaka and N. Mataga, *J. Phys. Chem.*, 1990, **94**, 5834.
- 5 (a) T. Asahi, M. Ohkohchi and N. Mataga, *J. Phys. Chem.*, 1993, **97**, 13132; (b) N. Mataga, H. Shioyama and Y. Kanda, *J. Phys. Chem.*, 1987, **91**, 314; (c) S. Ojima, H. Miyasaka and N. Mataga, *J. Phys. Chem.*, 1990, **94**, 7534; (d) H. Miyasaka, T. Nagata, M. Kiri and N. Mataga, *J. Phys. Chem.*, 1992, **96**, 8060; (e) T. Asahi and N. Mataga, *J. Phys. Chem.*, 1989, **93**, 6575; (f) T. Asahi, M. Ohkohchi, R. Matsusaka, N. Mataga, R. P. Zhang, A. Osuka and K. Maruyama, *J. Am. Chem. Soc.*, 1993, **115**, 5665; (g) T. Asahi and N. Mataga, *J. Phys. Chem.*, 1991, **95**, 1956.
- 6 J. Q. Chambers, *The Chemistry of Quinoid Compounds, Part 2*, ed. S. Patai, Wiley & Sons, New York, 1974; p. 737; and references cited therein.
- 7 (a) D. Rehm and A. Weller, *Isr. J. Chem.*, 1970, **8**, 259; (b) H. Leonhardt and A. Weller, *Ber. Bunsenges. Phys. Chem.*, 1963, **67**, 791.
- 8 N. J. Bunce, *The Chemistry of Quinoid Compounds, Part 1*, ed. S. Patai, Wiley & Sons, New York, 1974, p. 465; and references cited therein.

- 9 N. A. Shcheglova, D. N. Shigorin, G. G. Yakobson and L. S. Tushishvili, *Russ. J. Phys. Chem.*, 1969, **43**, 1112.
- 10 H. A. Benesi and J. H. Hildebrand, *J. Am. Chem. Soc.*, 1949, **71**, 2703.
- 11 S. P. Pappas, B. C. Pappas and N. A. Portnoy, *J. Org. Chem.*, 1969, **34**, 520.
- 12 C. Covell, A. Gilbert and C. Richter, *J. Chem. Res. (S)*, 1998, 316.
- 13 (a) E. Paterno and G. Chieffi, *Gazz. Chim. Ital.*, 1909, **39**, 341; (b) G. Büchi, C. G. Inman and E. S. Lipinski, *J. Am. Chem. Soc.*, 1954, **76**, 4327.
- 14 For general reviews on the Paterno-Büchi reactions, see: (a) G. Jones, II, *Organic Photochemistry*, ed. S. Padwa, Marcel Dekker, New York, 1981; vol. 5, p. 1–122; (b) A. G. Griesbeck, *CRC Handbook of Organic Photochemistry and Photobiology*, ed. W. M. Horspool and P.-S. Song, CRC Press, Boca Raton, Florida, 1995, p. 522; (c) D. R. Arnold, *Adv. Photochem.*, 1968, **6**, 301.
- 15 N. Haga, H. Takayaangi and H. Tokumaru, *Chem. Lett.*, 2001, 448.
- 16 (a) D. Sun, S. M. Hubig and J. K. Kochi, *J. Org. Chem.*, 1999, **64**, 2250; (b) E. Bosch, S. M. Hubig and J. K. Kochi, *J. Am. Chem. Soc.*, 1998, **120**, 386; (c) Y. Takahashi and J. K. Kochi, *Chem. Ber.*, 1988, **121**, 253.
- 17 P. S. Mariano and J. L. Stavinoha, *Synthetic Organic Chemistry*, ed. W. M. Horspool, Plenum Press, New York, 1984, p. 145.
- 18 E. Baciocchi, T. Del Giacco, F. Eleisei and M. J. Ioele, *J. Org. Chem.*, 1995, **60**, 7974.
- 19 (a) Y. Takahashi, F. Endoh, H. Ohaku, K. Wakamatsu and T. Miyashi, *J. Chem. Soc., Chem. Commun.*, 1994, 1127; (b) T. Miyashi, A. Konno, Y. Takahashi, A. Kaneko, T. Suzuki and T. Mukai, *Tetrahedron Lett.*, 1989, **30**, 5297; (c) T. Suzuki, Y. Yamashita, T. Mukai and T. Miyashi, *Tetrahedron Lett.*, 1988, **29**, 1405.
- 20 K. Maruyama and H. Imahori, *J. Org. Chem.*, 1989, **54**, 2692.
- 21 (a) J.-H. Xu, L.-C. Wang, J.-W. Xu, B.-Z. Yan and H. C. Yuan, *J. Chem. Soc., Perkin Trans. 1*, 1994, 571; (b) J.-H. Xu, Y.-L. Song, Z.-G. Zhang, L.-C. Wang and J.-W. Xu, *Tetrahedron*, 1994, **50**, 1199.
- 22 (a) S. S. Kim, D. Y. Yoo, I. H. Cho and S. C. Shim, *Bull. Korean Chem. Soc.*, 1987, **8**, 296; (b) S. S. Kim, D. Y. Yoo, A.-R. Kim and I. H. Cho, *Bull. Korean Chem. Soc.*, 1989, **10**, 66.
- 23 (a) M. Christl and M. Braun, *Angew. Chem.*, 1989, 636; (b) M. Christl and M. Braun, *Liebigs Ann./Recl.*, 1997, 1135.
- 24 Z. V. Todres, K. I. Dyusengaliev, M. M. Buzlanova, V. E. Shklover and Y. T. Struchkov, *J. Org. Chem. USSR*, 1990, **26**, 724.
- 25 G. O. Schenck, *Z. Electrochem.*, 1960, **64**, 997.
- 26 A. J. Barltrop and B. Hesp, *J. Chem. Soc. (C)*, 1967, 1625.
- 27 K. Ogino, T. Matsumoto and S. Kozuka, *J. Chem. Soc., Chem. Commun.*, 1979, 643.
- 28 N. Ishine, K. Hashimoto and Y. Yamaguchi, *J. Chem. Soc., Perkin Trans. 1*, 1975, 318.
- 29 (a) A. Samanta, C. Devadoss and R. W. Fessenden, *J. Phys. Chem.*, 1990, **94**, 7106; (b) R. Dunsbach and R. Schmidt, *J. Photochem. Photobiol. A: Chem.*, 1994, **83**, 7; (c) T. M. Siegel and H. B. Mark, Jr., *J. Am. Chem. Soc.*, 1972, **94**, 9020.
- 30 A. Samanta and R. W. Fessenden, *J. Phys. Chem.*, 1989, **93**, 5823.
- 31 N. Haga, H. Takayanagi and K. Tokumaru, *J. Org. Chem.*, 1997, **62**, 3734.
- 32 K. Kikuchi, M. Hoshi, E. Abe and H. Kokubun, *J. Photochem. Photobiol. A: Chem.*, 1988, **45**, 1.
- 33 J. Olmsted, III and T. J. Meyer, *J. Phys. Chem.*, 1987, **91**, 1649.
- 34 U. E. Steiner, H.-J. Wolff and T. Ohno, *J. Phys. Chem.*, 1989, **93**, 5147.
- 35 Y. Nishimura, H. Sakuragi and K. Tokumaru, *Bull. Chem. Soc. Jpn.*, 1992, **65**, 2887.
- 36 (a) G. Jones, II, W. A. Haney and X. T. Phan, *J. Am. Chem. Soc.*, 1988, **110**, 1922; (b) G. Jones, II, N. Mouli, W. A. Haney and W. R. Bergmark, *J. Am. Chem. Soc.*, 1997, **119**, 8788.
- 37 P. R. Hammond, *J. Chem. Soc.*, 1964, 471–479.
- 38 (a) H. J. Kuhn, S. E. Braslavsky and R. Schmidt, *Pure Appl. Chem.*, 1989, **61**, 188; (b) S. L. Murov, I. Carmichael and G. L. Hug, *Handbook of Photochemistry*, Marcel Dekker, Inc., New York, 1993; p. 298.
- 39 N. Haga, Y. Kuriyama, H. Takayanagi, H. Ogura and K. Tokumaru, *Photochem. Photobiol.*, 1995, **61**, 557.
- 40 J. G. Calvert and J. N. Pitts, Jr., *Photochemistry*, John Wiley & Sons, Inc., New York, 1966, p. 737.
- 41 TEXRAY Structure Analysis Package, Molecular Structure Corporation, 1985–1999.
- 42 (a) T. D. Santa Cruz, D. L. Akins and R. L. Birke, *J. Am. Chem. Soc.*, 1976, **98**, 1677; (b) I. Tanimoto, K. Kushioka and K. Maruyama, *Bull. Chem. Soc. Jpn.*, 1979, **52**, 3586.